Inorg. Chem. **2009**, *48*, 3047−3056

Identification by NMR Spectroscopy of the Two Stereoisomers of the Platinum Complex [$PtCl_2$(*S*-ahaz)] (*S*-ahaz = 3(*S*)-Aminohexahydroazepine) Bound to a DNA 14-mer Oligonucleotide. NMR Evidence of Structural Alteration of a Platinated A·T-rich 14-mer DNA Duplex

Connie I. Diakos,[†] Barbara A. Messerle,[‡] P. del Socorro Murdoch,[§] John A. Parkinson,[§,⊥] Peter J. Sadler,[||] Ronald R. Fenton,[†] and Trevor W. Hambley*[,†]

School of Chemistry, University of Sydney, NSW 2006, Australia, School of Chemical Sciences, University of New South Wales, NSW 2052, Australia, Department of Chemistry, University of Edinburgh, King's Buildings, West Mains Road, Edinburgh EH9 3JJ, U.K., Department of Chemistry, University of Warwick, Coventry CV4 7AL, U.K. and WestCHEM, Department of Pure and Applied Chemistry, University of Strathclyde, 16 Richmond Street, Glasgow, U.K.

Received November 18, 2008

The enantiomers of the asymmetric, chiral platinum(II) complex [$PtCl_2$(*S*-ahaz)] (*S*-ahaz = 3(*S*)-aminohexahydroazepine) each form two stereoisomers on binding to GpG sequences of DNA: one in which the primary amine is directed toward the 5′ end of the DNA and one in which it is directed toward the 3′ end. Previous binding studies have revealed that the *S*-enantiomer forms the two stereoisomers in a 7:1 ratio while the *R*-enantiomer forms them in close to a 1:1 ratio. In an attempt to elucidate the reasons behind the stereoselectivity displayed by the *S*-enantiomer and to establish which isomer is formed in the greater amount, we report here its reaction with a 14-mer oligodeoxyribonucleotide having a single GpG site. The two stereoisomers that formed were separated using HPLC methods, and their integrities were confirmed by electrospray ionization mass spectrometry. The DNA duplex was formed by combination of each of the purified reaction products with the complementary strand of DNA. Identification of both of the stereoisomers was achieved using 2D NMR spectroscopy, which is the first time this has been achieved for an unsymmetric platinum complex bound to DNA. The minor stereoisomer, with the bulk of the ahaz ring directed toward the 3′ end of the platinated strand, induced considerable disruption to the 14-mer DNA duplex structure. The primary amine of the ahaz ligand was oriented toward the 3′ side of the duplex in the major isomer, giving a DNA structure that was less disrupted and was more akin to the structure of the DNA on binding of cisplatin to the same sequence.

Introduction

The platinum compounds typified by cisplatin (*cis*-[$PtCl_2(NH_3)_2$]) are arguably the most widely used group of anticancer agents in the world and are undergoing a resurgence in use and development.[1] The d(GpG) intrastrand adduct formed by cisplatin on duplex DNA is by far the major adduct formed and is believed to be responsible for most of its anticancer activity.[2−9] The alteration to the DNA

* To whom correspondence should be addressed. E-mail: t.hambley@chem.usyd.edu.au. Telephone: +61-2-9351-2830. Fax: +61-2-9351-3329.
[†] University of Sydney.
[‡] University of New South Wales.
[§] University of Edinburgh.
[⊥] University of Strathclyde.
[||] University of Warwick.

(1) Kelland, L. R. *Nat. Rev. Cancer* **2007**, *7*, 573–584.
(2) Corda, Y.; Anin, M.-F.; Leng, M.; Job, D. *Biochemistry* **1992**, *31*, 1904–1908.
(3) Bradley, L. J. N.; Yarema, K. J.; Lippard, S. J.; Essigmann, J. M. *Biochemistry* **1993**, *32*, 982–988.
(4) Reed, E.; Ozols, R. F.; Tarone, R.; Yuspa, S. H.; Poirier, M. C. *Proc. Natl. Acad. Sci. U.S.A.* **1987**, *84*, 5024–5028.
(5) Comess, K. M.; Burstyn, J. N.; Essigmann, J. M.; Lippard, S. J. *Biochemistry* **1992**, *31*, 3975–3990.
(6) Corda, Y.; Job, C.; Anin, M.-F.; Leng, M.; Job, D. *Biochemistry* **1991**, *30*, 222–230.
(7) Hambley, T. W. *J. Chem. Soc., Dalton Trans.* **2001**, 2711–2718.

10.1021/ic802207m CCC: $40.75
Published on Web 03/05/2009

structure induced by the coordinative binding of the drug is thought to be responsible for this antitumor activity. Work with HMG (high mobility group) domain proteins has shown that they are able to recognize and bind to DNA bent by cisplatin bound to the GpG sequence[10−12] and they may be associated with interfering with repair processes that lead to resistance to the drug.[13,14] It is for reasons such as these that ascertaining the modifications to the DNA structure caused by platinum drugs is of such importance.

Structural studies of cisplatin DNA 1,2-intrastrand adducts have revealed several distinctive structural features.[12,15−28] Briefly, the most notable of these are the bend angle of the DNA, the canting angle between the platinated guanine bases, and the out-of-plane deformation of the platinum atom from the plane of the two bound guanines. Also typical of these structures are the sugar puckers of the platinated guanosines: the bifunctional adduct induces the sugar of the 5′ guanine to adopt the C_3' endo conformation that is more common in A-DNA, while the sugar of the 3′ guanine retains the C_2' endo conformation that is typical of B-DNA. Sadler et al. have determined the structure of the adduct formed by cisplatin with a 14-mer DNA duplex.[19] This 14 base-pair duplex is over one turn in length and has the following A•T pair rich sequence:

$$5'\text{-d}(A_1T_2A_3C_4A_5T_6G_7G_8T_9A_{10}C_{11}A_{12}T_{13}A_{14})\text{-}3'$$

$$3'\text{-d}(T_{28}A_{27}T_{26}G_{25}T_{24}A_{23}C_{22}C_{21}A_{20}T_{19}G_{18}T_{17}A_{16}T_{15})\text{-}5'$$

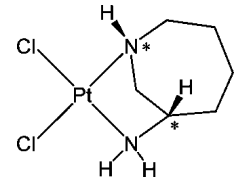

Figure 1. The [$PtCl_2$(*S*-ahaz)] complex. Chiral centers are denoted by an asterix.

This sequence has been used here to allow for a direct comparison between the effects of cisplatin and the bulkier platinum drugs upon the duplex DNA structure.

The asymmetric [$PtCl_2$(*S*-ahaz)] complex (Figure 1) has demonstrated high stereoselectivity in the formation of the 1,2-intrastrand adduct on binding to DNA.[29−31] Work on the complex bound to the dinucleotide d(GpG) combining 2D NMR spectroscopy and molecular mechanics modeling of an oligonucleotide adduct indicated a steric basis for this stereoselectivity, but it was not possible to definitively identify which isomer was the dominant one.[32] Here, we report on the effect of coordination of this complex to the 14-mer DNA duplex used by Sadler et al. as revealed by NMR spectroscopy through identification of the stereoisomers and determination of structural features.

Experimental Methods

Instrumentation. UV−vis measurements were carried out on a Shimadzu UV-2501PC UV−vis recording spectrometer or a Perkin-Elmer UV−vis Lambda 16 spectrometer with Uvwinlab software. High performance liquid chromatography (HPLC) separation was carried out on a bioCAD Sprint perfusion chromatography system (PerSeptive Biosystems) using a Nucleosil 300-5C8 semipreparative C8 reverse-phase stainless steel column, 25 cm × 7.75 mm i.d., 300 Å (Hichrom, U.K.). Positive and negative ion electrospray ionization mass spectrometry (ESI-MS) experiments were performed on a Platform II mass spectrometer (Micromass, Manchester, U.K.). The acquisition and deconvolution of data were performed on a Mass Lynx (V 2.3) Windows NT PC data system using the MaxEnt Electrospray software algorithm. The pH measurements were made using a Corning 145 pH meter equipped with an Aldrich combination electrode and a Hannah Instruments pH meter calibrated with Aldrich buffer solutions of pH 4, 7, and 10. Values of pH were adjusted with 1 M $HClO_4$ or NaOH as appropriate. NMR experiments were carried out on a Bruker DMX 500 MHz NMR spectrometer using a TBI [^{1}H, ^{13}C, X] probe head equipped with a z-field gradient coil, a Varian ^{Unity}INOVA spectrometer at 600 MHz using a triple-resonance probe head [^{1}H, ^{13}C, ^{15}N] equipped with z-field gradients, and a Bruker Avance DMX 600 MHz spectrometer using a TXI triple-resonance probe head equipped with triple-axis gradients. 2D NMR spectra were acquired in phase-sensitive mode with time-proportional phase incrementation. Spectra were acquired and processed with Bruker XWinNMR software, version 2.6. All spectra were referenced to the methyl singlet of TSP at 0 ppm.

Preparation of the [Pt(14-mer)(*S*-ahaz)] Adducts. Samples of a sufficient concentration for NMR analysis were prepared by first

(8) Jamieson, E. R.; Lippard, S. J. *Chem. Rev.* **1999**, *99*, 2467–2498.
(9) Ober, M.; Lippard, S. J. *J. Am. Chem. Soc.* **2008**, *130*, 2851–2861.
(10) Donohue, B. A.; Augot, M.; Bellon, S. F.; Treiber, D. K.; Toney, J. H.; Lippard, S. J.; Essigmann, J. M. *Biochemistry* **1990**, *29*, 5872–5880.
(11) Pil, P. M.; Lippard, S. J. *Science* **1992**, *256*, 234–236.
(12) Ohndorf, U.-M.; Rould, M. A.; He, Q.; Pabo, C. O.; Lippard, S. J. *Nature* **1999**, *399*, 708–712.
(13) Huang, J.-C.; Zamble, D. B.; Reardon, J. T.; Lippard, S. J.; Sancar, A. *Proc. Natl. Acad. Sci. U.S.A.* **1994**, *91*, 10394–10398.
(14) Zamble, D. B.; Mu, D.; Reardon, J. T.; Sancar, A.; Lippard, S. J. *Biochemistry* **1996**, *35*, 10004–10013.
(15) Herman, F.; Kozelka, J.; Stoven, V.; Guittet, E.; Girault, J.-P.; Huynh-Dinh, T.; Igolen, J.; Lallemand, J.-Y.; Chottard, J.-C. *Eur. J. Biochem.* **1990**, *194*, 119–133.
(16) Yang, D.; van Boom, S. S. G. E.; Reedijk, J.; van Boom, J. H.; Wang, A. H.-J. *Biochemistry* **1995**, *34*, 12912–12920.
(17) Gelasco, A.; Lippard, S. J. *Biochemistry* **1998**, *37*, 9230–9239.
(18) Dunham, S. U.; Dunham, S. U.; Turner, C. J.; Lippard, S. J. *J. Am. Chem. Soc.* **1998**, *120*, 5395–5406.
(19) Parkinson, J. A.; Chen, Y.; Murdoch, P. d. S.; Guo, Z.; Berners-Price, S. J.; Brown, T.; Sadler, P. J. *Chem.−Eur. J.* **2000**, *6*, 3636–3644.
(20) Marzilli, L. G.; Saad, J. S.; Kuklenyik, Z.; Keating, K. A.; Xu, Y. *J. Am. Chem. Soc.* **2001**, *123*, 2764–2770.
(21) Sherman, S. E.; Gibson, D.; Wang, A. H.-J.; Lippard, S. J. *Science* **1985**, *230*, 412–417.
(22) Sherman, S. E.; Gibson, D.; Wang, A. H.-J.; Lippard, S. J. *J. Am. Chem. Soc.* **1988**, *110*, 7368–7381.
(23) Takahara, P. M.; Rosenzweig, A. C.; Frederick, C. A.; Lippard, S. J. *Nature* **1995**, *377*, 649–652.
(24) Takahara, P. M.; Frederick, C. A.; Lippard, S. J. *J. Am. Chem. Soc.* **1996**, *118*, 12309–12321.
(25) Spingler, B.; Whittington, D. A.; Lippard, S. J. *Inorg. Chem.* **2001**, *40*, 5596–5602.
(26) Wu, Y. B.; Pradhan, P.; Havener, J.; Boysen, G.; Swenberg, J. A.; Campbell, S. L.; Chaney, S. G. *J. Mol. Biol.* **2004**, *341*, 1251–1269.
(27) Spingler, B.; Whittington, D. A.; Lippard, S. J. *Inorg. Chem.* **2001**, *40*, 5596–5602.
(28) Silverman, A. P.; Bu, W. M.; Cohen, S. M.; Lippard, S. J. *J. Biol. Chem.* **2002**, *277*, 49743–49749.
(29) Fenton, R. R.; Easdale, W. J.; Er, H. M.; O'Mara, S. M.; McKeage, M. J.; Russell, P. J.; Hambley, T. W. *J. Med. Chem.* **1997**, *40*, 1090–1098.
(30) Er, H. M., Ph.D. Thesis, The University of Sydney, Australia, 1996.
(31) Er, H. M.; Hambley, T. W. *J. Inorg. Biochem.* **2009**, *103*, 168–173.
(32) Diakos, C. I., Ph.D. Thesis, The University of Sydney, Australia, 2002.

forming the $[Pt(S\text{-ahaz})(OH_2)_2]^{2+}$ species. The complex $[PtCl_2(S\text{-ahaz})]$ was synthesized according to a published procedure.[29] A 5 mM solution of $[PtCl_2(S\text{-ahaz})]$ in H_2O (Sigma, double-processed tissue culture water) was mixed with 1.95 mol equiv of $AgNO_3$, stirred in the dark for 48 h, and then centrifuged at 10^4 rpm for 20 min. The solution was decanted and stored in the freezer until required. The 14-mer oligonucleotides, d(ATACATGGTACATA) ("GG strand") and d(TATGTACCATGTAT) ("CC strand"), were supplied as HPLC-purified sodium salts by Oswel (Southampton, U.K.). The [Pt(14-mer)(*S*-ahaz)] adducts were formed by mixing 1 mol equiv of the diaqua platinum species (469 μL, 5 mM) with the GG 14-mer strand (13.26 mL, 203 μM), and the sample was incubated at 310 K for 2 days. Addition of a second platinum equivalent was found to be necessary to ensure sufficient platination in previous experiments; therefore, a second equivalent was also added here, and the mixture was incubated for a further seven days.

HPLC Separation of the Isomers. The two isomers formed by the binding of the asymmetric platinum complex to the GG DNA strand were separated by HPLC. A mobile phase of 20 mM tetraethylammonium acetate and 50% acetonitrile (gradient: 18% acetonitrile for 10 min, 18−25% from 10 to 20 min, 25−18% from 20 to 22 min) was used with a flow rate of 1 mL min^{-1} at 298 K. The bands due to each isomer, S1 and S2, were collected separately and flash-frozen in liquid nitrogen as soon as the samples were removed from the HPLC to avoid reactions between the solvents and the DNA. The combined fractions were vacuum freeze-dried. The approximate concentration of the band samples was determined by UV−vis spectroscopy using the extinction coefficient for the unplatinated single-GG strand as an approximation in calculations (GG strand, millimolar extinction coefficient ϵ at 260 nm is 149.0 for an absorbance of 1 μmol in 1 mL; CC strand, ϵ at 260 nm is 137.2).

ESI-MS Methods. The integrity of the samples was confirmed by the use of ESI-MS. The samples for positive and negative ESI-MS experiments were infused at 10 μL min^{-1}, and the ions were produced in an atmospheric pressure ionization (API)/ESI ion source. The source temperature was 338 K, and the drying gas flow rate was 300 L h^{-1}. For positive ion ESI-MS, a potential of 3.5 kV was applied to the probe tip, and a cone voltage gradient of 50−90 V over 1000−2000 Da was used. The quadrupole was scanned at 100 amu s^{-1}.

Preparation of the NMR Samples. The NMR samples were made up in D_2O (Apollo Scientific Ltd., >99.92% D). Initial $1D^1H$ NMR experiments showed the presence of residual TEAA so the samples were lyophilized again in an unsuccessful attempt to remove this. Samples were redissolved in D_2O (0.5 mL ampule from Aldrich, 99.9 atom % D). The ionic strength was increased by adding $NaClO_4$ so as to give a 100 mM solution.

Formation of Platinated Duplex from [Pt(14-mer)(*S*-ahaz)]. The duplex was formed by titrating in approximately equimolar amounts of the CC strand (6.03 mM in D_2O) and by monitoring the duplex formation by $1D^1H$ NMR, with sharpening of resonances being indicative of duplex formation. For band S1 this required an addition of 35 μL of CC strand stock solution, and for band S2 an addition of 40 μL of the CC strand stock solution was needed. The NMR samples of the two bands had pH* values of 6.49 and 6.09, respectively, and were used without further pH adjustment.

NMR Spectroscopy Methods. NMR experiments were carried out on ca. 1.2 mM solutions of [Pt(14-mer)(*S*-ahaz)]. Spectra of S1 were initially collected at 298 K in D_2O at 500 MHz over a spectral width of 5000 Hz. Standard Bruker pulse sequences were used incorporating water suppression by presaturation. A 2D NOESY NMR spectrum was collected with a mixing time of 200 ms. Data sets resulting from 1024 increments of t_1 were acquired, with each free induction decay composed of 4096 data points. For each increment of t_1, 48 transients were recorded, with a recycle delay of 3.0 s. A 2D DQF-COSY NMR spectrum was acquired with data sets resulting from 800 increments of t_1 with each free induction decay composed of 4096 data points. For each increment of t_1, 80 transients were recorded.

All spectra of S2 and those from a 90% H_2O:10% D_2O solution of S1 were acquired at 600 MHz. 2D NMR NOESY spectra of both S1 and S2 were acquired with 90% H_2O:10% D_2O solutions using mixing times (τ_m) of 40, 80, 150, 300, and 600 ms at 298 K over a spectral width of 12 000 Hz. NOESY NMR spectra acquired with a mixing time of 150 ms were also collected at 280 K for both S1 and S2. A WATERGATE pulse sequence was employed for water suppression, followed by a flip-back sequence in the case of S1, but not S2. Data sets resulting from 800 increments of t_1 were acquired, with each free induction decay composed of 2048 data points. For each increment of t_1 either 96 or 104 transients were recorded. A recycle delay of 1.8 s was used. 2D DQF-COSY NMR spectra were recorded using a standard Bruker pulse sequence incorporating water suppression by presaturation, over a spectral width of 5500 Hz. Data sets resulting from 640 increments of t_1 were acquired, with each free induction decay composed of 2048 data points. For each increment of t_1, 128 transients were recorded. 2D COSY-45 NMR spectra were recorded using a standard Bruker pulse sequence incorporating water suppression by presaturation. 2D TOCSY NMR spectra were recorded using a standard Bruker clean TOCSY pulse sequence. TOCSY spectra were recorded with mixing times of 40 and 80 ms over a spectral width of 6600 Hz. Data sets resulting from 600 increments of t_1 were acquired with each free induction decay composed of 2048 data points. For each increment of t_1, 136 transients were recorded. All spectra were processed by zero-filling and by subjecting the data to shifted sine-bell weighting functions in F1 and F2 of $\pi/2$ prior to Fourier transformation and were baseline corrected using Bruker XWin-NMR software, version 2.6.

Results and Discussion

Preparation of the NMR Samples. Preparation of pure samples of platinated 14-mer isomers was carried out by gradient method reverse-phase HPLC (Supporting Information, Figure S1). The identity of the samples was confirmed by ESI-MS. The raw and deconvoluted mass spectra (Supporting Information, Figure S2) show the most abundant species to be at 4578.4 amu for band S1 (theoretical mass for [Pt(14-mer)(*S*-ahaz)] 4578.0 amu) and 4578.3 amu for band S2. The duplexes were formed by titrating in small aliquots of the CC strand to solutions containing the separated isomers on the GG strand. Duplex formation was monitored by $1D^1H$ NMR, with sharpening of resonances observed as the duplexes formed (Supporting Information, Figure S3). It was not necessary to anneal the duplexes.

Assignment of the NMR Spectra of the 14-mer Duplex. The resonances due to protons of the 14-mer duplex were assigned using the NOESY spectra following established methods for right-handed duplex DNA.[33,34] A walk was first

(33) Wüthrich, K. *NMR of Proteins and Nucleic Acids*; Wiley-Interscience: New York, 1986.
(34) Wijmenga, S. S.; Mooren, M. M. W.; Hilbers, C. W. In *NMR of Macromolecules. A Practical Approach*; Roberts, G. C. K., Ed.; Oxford University Press: Oxford, U.K., 1993; pp 217−288.

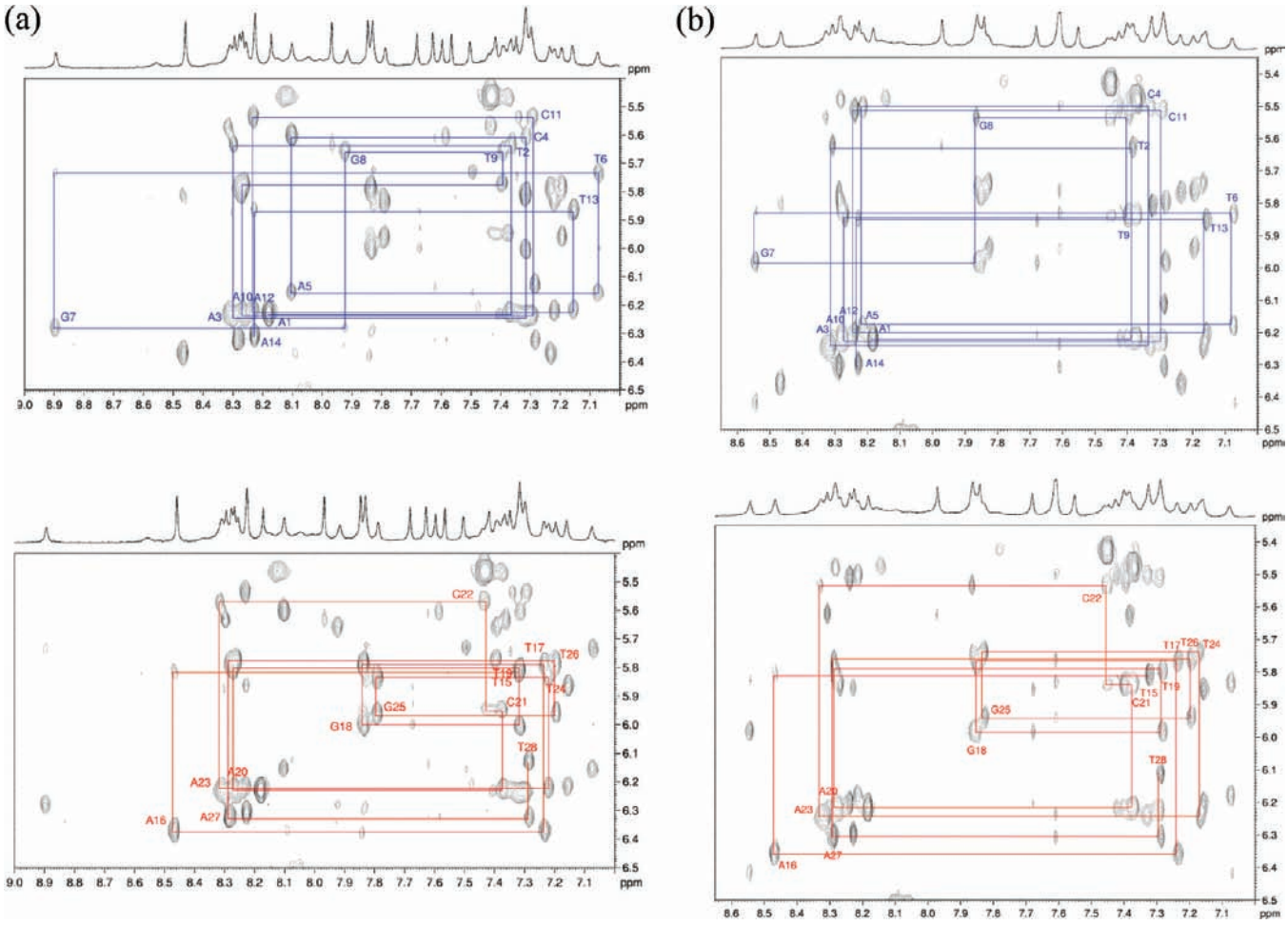

Figure 2. Duplicate contour plots of the base H8/H6 sugar H1′ resonance NOE cross-peak region for the platinated GG strand (top) and complementary strand (bottom) for (a) the S1 isomer and (b) the S2 isomer shown for NOESY NMR data acquired at a mixing time of 150 ms.

made from the base to sugar H1′ protons for each strand, starting at the terminal 5′ residues A1 and T15 for the GG and CC strands, respectively (Figure 2a for band S1 and Figure 2b for band S2). The H8/H6 protons of these 5′ bases show a connectivity only to the H1′ protons of their own sugar and, hence, are useful as the starting point. Sequential connectivities were then made from a base proton, H6 or H8, to its own sugar H1′ proton and then from that H1′ proton to the base that follows it in the 3′ direction, i.e., *n*H8/H6 to *n*H1′ and from *n*H1′ to (*n*+1)H8/H6. Weak cross-peaks were observed for many of the resonances due to interactions between adenosine H2 protons and interstrand, intranucleotide, and internucleotide H1′ sugar protons. Strong cross-peaks were seen for intranucleotide cytosine H5 and H6 protons.

Analogous NOESY assignment walks were made using the base H6/H8 and the sugar H2′, H2″ proton resonances and also the base aromatic and the sugar H3′ proton resonances. A complete walk around the duplex was possible for the 2′/2″ protons for both bands. For the H6/H8−H3′ walk, some disruptions were seen. In band S1 these were at the T13−A14 connection and the C22−A23 connection with the C22 H6−H3′ correlation absent. Similar disruptions were seen in band S2.

The thymine methyl protons were assigned using a combination of the H6 methyl contacts seen in the 2D COSY NMR spectra and the cross-peaks observed in the 2D NOESY NMR spectra. For band S1, the T6 methyl resonance is shifted far upfield. Interestingly for band S2, it was the T9 methyl resonance that shows an upfield shift of 0.3 ppm relative to band S1 (Figure 3). This may indicate alteration of the DNA structure involving movement of this methyl group away from an aromatic ring, most likely the A10 base. In Tables 1 and 2, the chemical shifts of all nonexchangeable protons are compiled for the 14-mer duplexes of bands S1 and S2, respectively.

Assignment of Sugar Resonances. The 2′ and 2″ sugar protons were assigned fully by examination of the relative cross-peak intensities of the H1′/H2′ and H1′/H2″ correlations in the 150 ms 2D NOESY NMR spectrum (see Supporting Information, Figure S4). The upfield proton was assigned as the 2′ proton and the downfield proton as the 2″ proton for all residues except A14, where the 2″ proton was found to be shifted upfield. In the case of the T28 residue, these two resonances were superimposed. Assignment of the 5′ and 5″ protons was made via Shugar and Remin's rule.[35]

(35) Remin, M.; Shugar, D. *Biochem. Biophys. Res. Commun.* **1972**, *48*, 636–642.

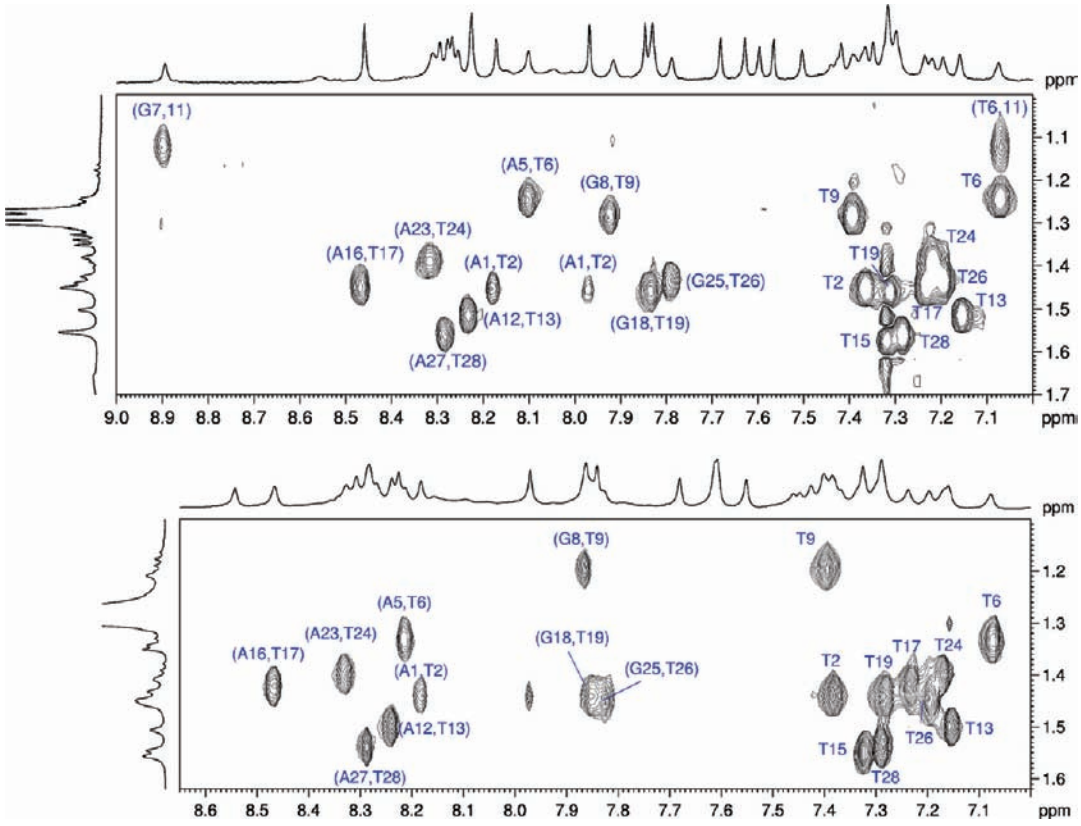

Figure 3. 2D NOESY NMR spectrum (τ_m = 150 ms, 298 K) detailing cross-peaks due to correlations between aromatic and thymine methyl proton resonances and aromatic ligand proton resonances for band S1 (top) and band S2 (bottom).

Table 1. ^{1}H Chemical Shifts (ppm) of the Platinated 14-mer Duplex Isolated as Band S1

base	H6/H8	H5/H2/CH_3	H1′	H2′	H2″	H3′	H4′	H5′/H5″	GH1/TH3	CH4b/H4f[a]
A1	8.18	7.97	6.23	2.68	2.83	4.88	4.28	4.11/3.82		
T2	7.37	1.46	5.65	2.18	2.46	5.03	4.23	4.15		
A3	8.30	7.61	6.24	2.76	2.90	5.06	4.46	4.22/4.11		
C4	7.32	5.32	5.62	2.24	2.44	4.82	4.27	4.20/3.98		8.07/6.57
A5	8.11	7.52	6.16	2.64	2.78	4.87	4.35	4.21/4.11		
T6	7.09	1.26	5.75	2.25	2.37	4.59	4.12	4.30/4.08	14.06	
G7	8.89		6.28	2.58	2.75	5.22	4.29	4.38/4.15		
G8	7.93		5.67	2.27	2.66	4.60	4.26	4.12/4.07	13.19	
T9	7.40	1.30	5.78	2.22	2.59	4.90	4.23	4.10	13.82	
A10	8.26	7.36	6.24	2.68	2.90	5.05	4.43	4.23		
C11	7.30	5.32	5.56	2.05	2.38	4.86	4.19	4.11/4.05		8.17/6.60
A12	8.23	7.69	6.22	2.60	2.84	5.00	4.40	4.20/4.09		
T13	7.17	1.52	5.87	1.93	2.28	4.81	4.12	4.19/4.03		
A14	8.23	7.56	6.30	2.68	2.47	4.73	4.22	4.13		
T15	7.33	1.58	5.83	1.81	2.23	4.68	4.03	3.74/3.67		
A16	8.47	7.85	6.37	2.90	3.04	5.04	4.48	4.15/4.07		
T17	7.24	1.45	5.81	2.21	2.51	4.82	4.29	4.21/3.71	13.33	
G18	7.84		6.01	2.64	2.79	4.95	4.40	4.29/4.21	12.45	
T19	7.33	1.46	5.82	2.25	2.57	4.92	4.42	4.26/4.19	13.49	
A20	8.28	7.43	6.23	2.61	2.83	5.03	4.39	4.23/3.90		
C21	7.38	5.35	5.95	1.95	2.37	4.74	4.12	4.29		8.58/6.90
C22	7.44	5.48	5.59	2.07	2.46	4.70	4.09	3.91		8.12/6.80
A23	8.32	7.84	6.23	2.76	2.90	5.05	4.34	4.16/3.99		
T24	7.23	1.40	5.84	2.23	2.49	4.93	4.28	4.22	13.32	
G25	7.79		5.97	2.58	2.75	4.97	4.40	4.29/4.20	12.27	
T26	7.21	1.44	5.80	2.04	2.44	4.90	4.17	4.21/4.10	13.50	
A27	8.28	7.63	6.32	2.76	2.88	5.03	4.43	4.25/4.19		
T28	7.29	1.56	6.13	2.18	2.18	4.55	4.07	4.37/3.92		

[a] CH4b for cytosine amino proton involved in H-bonding in CG base pair. CH4f for non-H-bonded amino proton.

2D TOCSY NMR spectra were used to confirm the assignment of the sugar protons 1′, 2′, 2″, 3′, 4′, 5′, and 5″. The 4′ sugar proton assignments were made from the 2D DQF-COSY NMR spectrum using the 3′−4′ connection. In some instances, a further connection step between the H4′ and H5′/H5″ proton resonances was possible.

Determination of Sugar Ring Conformation. The pucker of the sugars in this system was determined by examination

Table 2. ^{1}H Chemical Shifts (ppm) of the Platinated 14-Mer Duplex Isolated as Band S2

base	H6/H8	H5/H2/CH_3	H1′	H2′	H2″	H3′	H4′	H5′/H5″	GH1/TH3	CH4b/H4f
A1	8.19	7.97	6.23	2.68	2.83	4.89	4.28	3.81/3.64		
T2	7.39	1.46	5.64	2.19	2.46	4.90	4.22	4.15/4.11		
A3	8.31	7.62	6.25	2.75	2.90	5.06	4.46	4.21/4.13		
C4	7.33	5.33	5.52	2.10	2.39	4.84	4.40	4.19/3.99		8.10/6.54
A5	8.21	7.62	6.19	2.62	2.82	4.98	4.39	4.13/3.93		
T6	7.08	1.36	5.85	1.72	2.29	4.86	4.26	4.09	13.78	
G7	8.55		6.00	2.54	2.75	4.98	4.26	4.18/4.03		
G8	7.87		5.55	2.21	2.54	4.64	4.18	4.10/3.97		
T9	7.40	1.22	5.85	2.25	2.60	4.92	4.24	4.05	13.63	
A10	8.27	7.44	6.23	2.70	2.91	5.04	4.43	4.21/4.09		
C11	7.30	5.32	5.53	2.03	2.37	4.85	4.18	4.14		8.17/6.59
A12	8.24	7.69	6.21	2.60	2.83	5.00	4.40	4.19/4.13		
T13	7.16	1.52	5.86	1.92	2.27	4.83	4.12	4.20		
A14	8.23	7.55	6.31	2.67	2.47	4.72	4.21	4.12		
T15	7.33	1.57	5.82	1.80	2.23	4.67	4.03	3.75/3.66		
A16	8.47	7.84	6.37	2.89	3.03	5.04	4.47	4.14/4.06		
T17	7.24	1.44	5.78	2.19	2.50	4.90	4.28	4.20	13.34	
G18	7.85		6.00	2.64	2.78	4.96	4.42	4.20	12.45	
T19	7.29	1.46	5.81	2.16	2.53	4.92	4.42	4.26/4.10	13.51	
A20	8.28	7.42	6.23	2.69	2.87	5.04	4.43	4.20/4.08		8.14/6.82
C21	7.37	5.50	5.86	1.99	2.38	4.72	4.16	4.32/4.09		
C22	7.46	5.45	5.55	1.97	2.35	4.81	4.07	3.99/3.93		7.79/6.79
A23	8.33	7.87	6.26	2.77	2.93	5.04	4.40	4.13/3.94		
T24	7.17	1.42	5.75	2.14	2.45	4.89	4.39	4.22	13.35	
G25	7.83		5.95	2.60	2.74	4.96	4.40	4.22/4.16	12.41	
T26	7.20	1.47	5.78	2.01	2.41	4.88	4.16	4.21	13.50	
A27	8.29	7.61	6.31	2.76	2.88	5.03	4.42	4.21/4.11		
T28	7.29	1.56	6.12	2.19	2.19	4.54	4.06	4.30		

of several spectral features. In the 2D DQF-COSY NMR spectrum, a larger coupling of the 1′, 2′ protons is a feature of C_2′ endo (*S*-type) pucker, where the 1′, 2′ protons are trans with respect to one another. The presence of only a H3′/H2′ cross-peak of medium-strength coupling is also diagnostic of C_2′ endo puckering, with the very small (1−2 Hz) coupling of the H3′/H2″ proton pair leading to a cross-peak generally too weak in intensity to be observable.[33,36] The reverse of these features is seen in the C_3′ endo (*N*-type) pucker characteristic of A-DNA. Additionally, in the 150 ms 2D NOESY NMR spectrum, a weaker cross-peak consistent with a longer (∼4−4.5 Å) distance from the base proton to its 3′ sugar also indicated a C_2′ endo pucker, as opposed to a short (∼2.8−3 Å) distance in C_3′ endo puckering.

From examination of the 2D DQF-COSY NMR spectra (see Supporting Information, Figure S5), the pucker of all sugars of band S1, with the exception of those of T6, G7, and C21 was determined as being C_2′ endo. The 2D DQF-COSY NMR spectrum of band S2 indicated that all sugar puckers were C_2′ endo, with the exception of G7, and the T6 sugar is in a *N*↔*S* equilibrium.

Effect of Platination on Duplex Resonances. The H8 signals for the two platinated guanine bases, G7 and G8, of both bands are shifted downfield relative to those of the nonplatinated duplex.[19] The effect is more pronounced for band S1 than band S2 (Table 3). Strong cross-peaks are seen between the resonances due to these two protons in both molecules, indicating destacking of the two purine bases as a result of platinum coordination, with tilting of the bases toward one another. This effect has been seen previously in NMR studies of duplexes platinated at adjacent GG sites by cisplatin.[17,19]

Table 3. ^{1}H NMR Chemical Shifts (ppm) of the G7 and G8 H8 Signals of Bands S1, S2, and the Unplatinated 14-mer[19]

structure	G7 H8 (ppm)	G8 H8 (ppm)
unplatinated 14-mer	7.75	7.56
band S1	8.89	7.93
band S2	8.55	7.87
cisplatin	8.64	8.08

It is now a well-established characteristic of bifunctional 1,2-intrastrand platinated DNA cross-links that the sugar of the 5′-platinated purine nucleotide is distorted into the C_3′ endo pucker characteristic of A-DNA. A strong H8−H3′ cross-peak in the 150 ms NOESY NMR spectrum of band S1 (see Supporting Information, Figure S6) together with inspection of the coupling strengths of the relevant COSY cross-peaks confirmed this assignment for G7. It is also a well-noted feature of B-DNA in solution that the 3′ terminal residue often adopts a C_3′ endo pucker. This was not seen here for the platinated GG strand terminus of A14. It was not possible to determine whether this was a feature of the 3′ terminal sugar of the CC strand (associated with T28) since the H2′ and H2″ proton resonances were coincident in the NMR spectrum. The same data also showed that the sugar ring of T6 exists in a predominantly C_3′ endo conformation. The structure of the cisplatin adduct reported by Sadler et al. indicated that the sugar of T6 was in a *N*↔*S* equilibrium,[19] but the spectra for the platinated duplex investigated here implied that the T6 sugar is closer to being *N*-type. The distortion of the C21 sugar ring to a C_3′ endo pucker conformation, while unique in structures of bifunctional intrastrand platinum adducts determined thus far (with the exception of one[20]), is not completely surprising as this base lies opposite to the platinated lesion and some disruption is expected. These features can be seen in the section of the 2D COSY NMR spectrum (shown in Supporting Information,

(36) Altona, C. *Recl: J. R. Neth. Chem. Soc.* **1982**, *101*, 413–433.

Figure S5). Band S2 by contrast showed less duplex conformation distortion, with the G7 sugar ring also being twisted into a C_3' endo pucker but that of C21 remaining C_2' endo and that of T6 being in an $N \leftrightarrow S$ equilibrium.

Assignment of Exchangeable Protons. The exchangeable imino protons of the G and T bases were assigned using 2D NOESY NMR spectra recorded for a 90% H_2O:10% D_2O solution. The imino-to-imino proton NOE cross-peak region is presented in Figure 4 for NMR spectra acquired at 280 K. Assignment of the individual protons was made by a sequential walk from adjacent G to T bases, intra- and interstrand, via a chain of connectivities involving the exchangeable protons associated with Watson−Crick hydrogen bonding of base pairs. This sequence of connectivities was interrupted only at the T6-G7-G8 step. Assignments were additionally confirmed by the existence of NOE contacts between imino protons and A H2 or C H5 protons. The resonances expected for the imino proton associated with the A1·T28 base pair and for the T13·A16 and T14·A15 base pairs were absent from the spectrum of band S1.

For band S2, it was possible to assign many of the imino protons of the G and T bases from the 2D NOESY NMR spectrum recorded at 298 K. However, a spectrum was again recorded at 280 K to allow observation of a fuller complement of peaks. Even at this temperature, it was not possible to observe as many of the connections as were seen in band S1, indicating a different exchange regime for some of the NH protons of band S1. The imino proton resonance region measured of this 280 K spectrum is presented in Figure 4, and chemical shifts are listed in Table 4.

DNA Melting Point. The greatest resolution of the imino proton resonances was observed to occur at lower temperatures. For this reason, NMR data acquired at 280 K were used to assign the fullest complement of imino proton resonances. A melting point study was undertaken for band S1, and the duplex melted at between 318 and 323 K as evidenced by the disappearance of the imino proton resonances through intermediate exchange broadening (see Supporting Information, Figure S7). At lower temperatures, 11 imino proton resonances were visible in the NMR data. These represent the 10 central base-pair resonances observed in the 2D NOESY NMR spectrum with the addition of the imino proton resonance of T13 being present, thereby extending the assignment walk among exchangeable protons to one step further along the 3′ direction of the GG strand.

Examination of the imino proton resonance region of the ^{1}H NMR spectrum over the temperature range 278−323 K (see Supporting Information, Figure S7) provided information on the relative rates at which imino proton resonances undergo exchange. Upon heating the duplex to 298 K, the first resonance to disappear was that of the G7 imino proton. This is an illustration of the strain induced by the bifunctional platinum lesion at its 5′ end. With further heating, the T6 imino proton resonance began to undergo exchange broadening, which is a further indication of the strain at this end of the platinum lesion. The intensity of the G25 imino proton resonance also began to fall. This base is paired with C4, and the data showed the relative instability of the structure

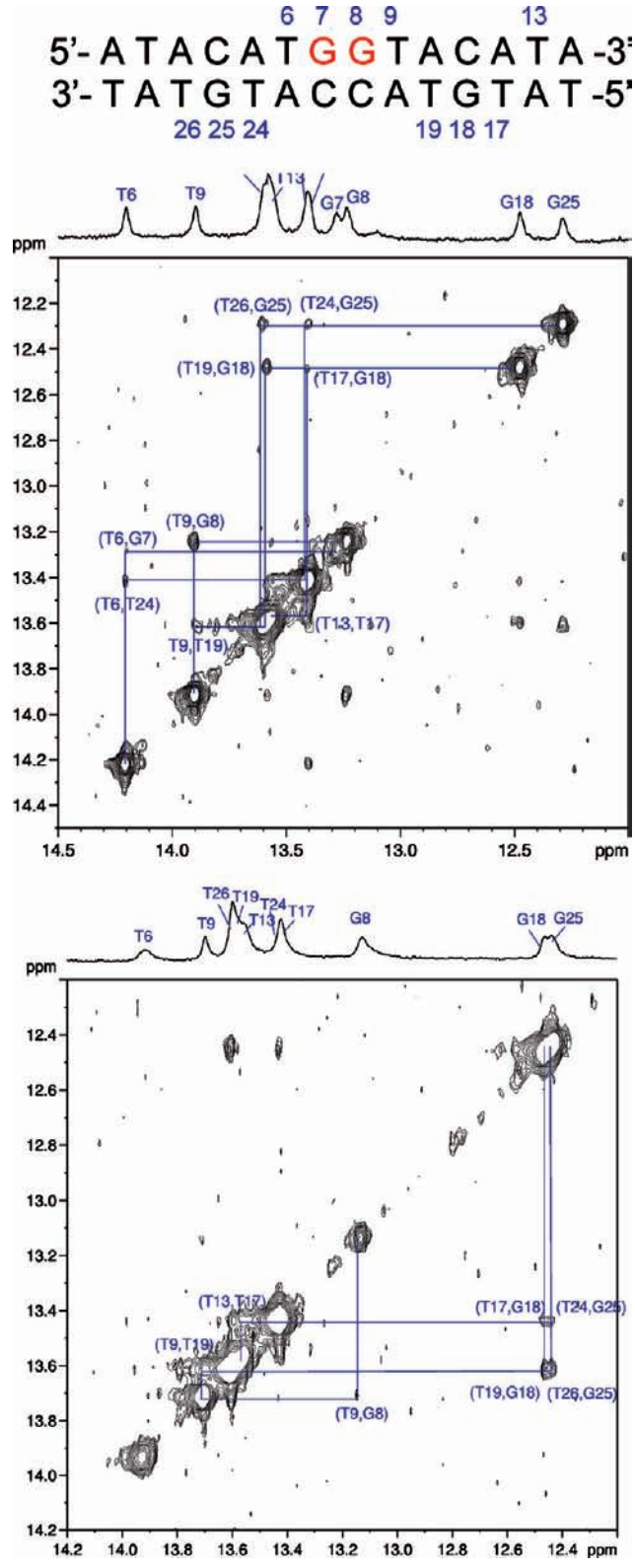

Figure 4. Imino proton to imino proton resonance cross-peak region showing the sequential walk between G and T bases for (top) band S1 and (bottom) band S2. NOESY NMR data were acquired on samples solubilized in 90% H_2O:10% D_2O with a mixing time $\tau_m = 150$ ms and were regulated at a probe temperature of 280 K.

further along the duplex 5′ to the platinated adduct. The two most stable base pairs, as indicated by their persistent imino proton resonances, are those of the G8·C21 and T9·A20

Table 4. Chemical Shifts of the Imino Protons from the NOESY Spectra (τ_m = 150 ms NOESY, 280 K) for Bands S1 and S2

base	band S1 GH1/TH3	band S2 GH1/TH3
T2	–	–
T6	14.20	13.92
G7	13.28	–
G8	13.23	13.13
T9	13.90	13.71
T13	13.56	13.56
T15	–	–
T17	13.41	13.43
G18	12.47	12.46
T19	13.57	13.60
T24	13.40	13.44
G25	12.29	12.44
T26	13.60	13.61
T28	–	–

pairs, which is consistent with a greater relative stability of the duplex structure 3′ to the platinated lesion.

Assignment of Resonances Due to the Ahaz Ligand. A combination of the 2D [^{1}H, ^{1}H] DQF-COSY, TOCSY, and NOESY NMR spectra was employed to obtain a full assignment of the resonances due to the ahaz ligand protons. Ligand assignment ideally stems from the identification of five geminal pairs of proton signals from the COSY NMR spectrum with a correlation to the resonance of the unpaired eleventh proton. For band S1, the COSY NMR spectrum clearly showed the expected number of geminal pairs (see Supporting Information, Figure S8). Additional correlations were made using the clean TOCSY NMR spectrum (Figure 5), with full assignment being made using a combination of the 2D TOCSY and NOESY NMR spectra. The endocyclic NH and exocyclic NH_2 protons were assigned using the NOESY NMR spectrum. The assignments of the ligand proton resonances are presented in Table 5. Figure 6 illustrates the position of the protons on the ligand ring.

Assignment of the ligand proton NMR resonances for band S2 was made primarily from a combination of the clean TOCSY NMR data (τ_m = 40 ms) and the DQF-COSY NMR data. The latter showed only five correlations; as for band S1, these were due to the five geminal pairs. The TOCSY NMR data allowed correlations to be made around the ahaz seven-membered ring (Figure 5). The NOESY NMR spectra showed resonances consistent with this assignment. The resonance assignments are presented in Table 5 for band S2, with their positions on the ahaz ring illustrated in Figure 1. The pattern of resonances is very similar to that observed for band S1. The exception is proton 11 in band S1, which is shifted far upfield compared with the equivalent resonance for band S2, implying close proximity edge-on association with an aromatic base.

Identification of the Stereoisomers. The orientation of the {Pt(*S*-ahaz)}$^{2+}$ moiety relative to the DNA duplex for each band was determined using the cross-peaks in the NOESY NMR spectra that indicated close proximity ligand−nucleotide contacts. The contacts that led to this assignment are presented in Table 6 for the τ_m = 150 ms NOESY NMR data. The contacts are illustrated on a molecular model as shown in Figure 7 and schematically in Supporting Information, Figure S9. This NOESY NMR spectrum was acquired with a mixing time long enough to

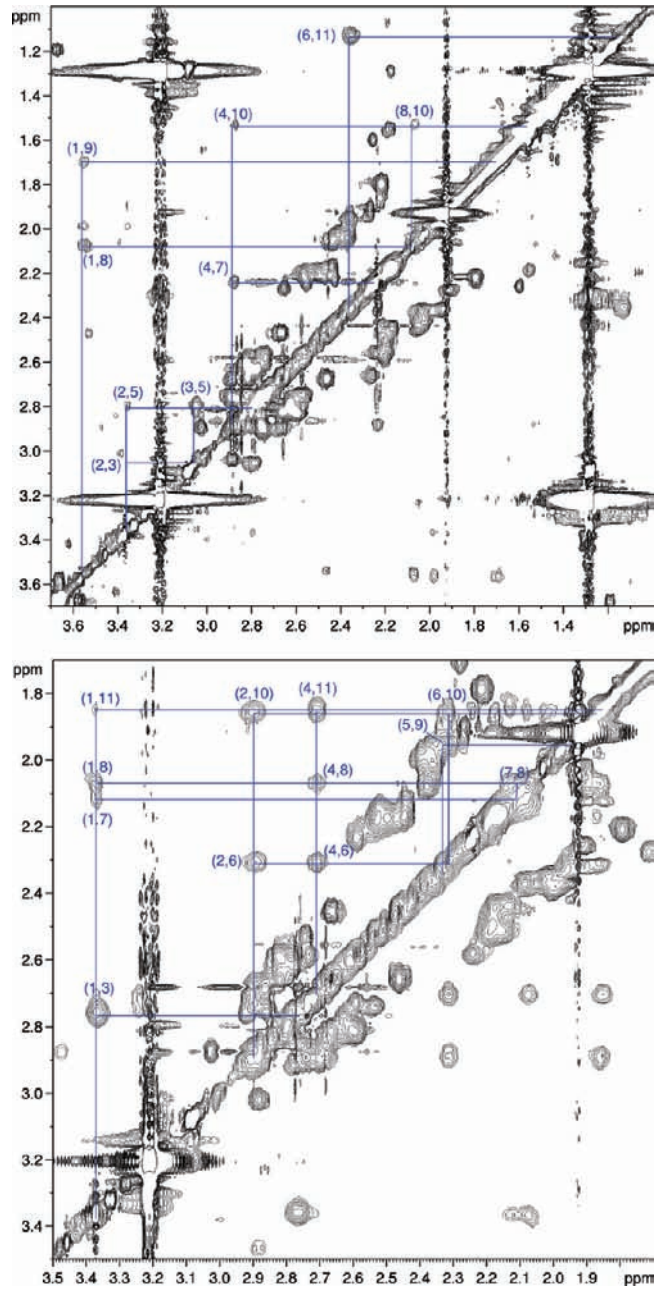

Figure 5. Clean TOCSY NMR spectrum (τ_m = 40 ms) for band S1 (top) and band S2 (bottom) detailing ligand resonances with connections between them marked.

allow for evolution of the ligand−DNA through-space contacts, but without the misleading correlations that result from spin diffusion, which might be present in NOESY NMR spectra acquired with longer mixing times. The approximate interproton distances listed in Table 6 were calculated using the isolated spin-pair approximation method based on intensities measured in the τ_m = 150 ms NOESY spectrum.

Band S1 of the [Pt(*S*-ahaz)(14-mer)] complex was assigned as the stereoisomer in which the primary amine is directed toward the 3′ side of the DNA (Figure 6), primarily based on the large number of contacts made by ligand proton 11 with the T6 and G7 bases. It is also consistent with the large upfield shift of the resonance due to this proton on the ligand binding to DNA. In this orientation, the ligand ring is adjacent to the 5′ side of the GG strand, with its bulk

Table 5. Chemical Shifts of the ahaz Ligand Protons (ppm) for Bands S1 and S2

ligand proton	band S1 (ppm)	band S2 (ppm)
1	3.57	3.37
2	3.35	2.90
3	3.07	2.77
4	2.87	2.71
5	2.78	2.32
6	2.35	2.31
7	2.24	2.13
8	2.08	2.08
9	1.72	1.96
10	1.52	1.87
11	1.13	1.85
endo NH	6.94	6.65
exo NH_2	6.16	6.43

extended out into the major groove. The endocyclic amine proton showed a contact to the G7 H8 proton. The *R*-chirality of the endocyclic nitrogen forces its proton to be "up" with respect to the platinum plane, allowing for this contact to take place. [Note: The platinum plane direction is defined with respect to the H8 atoms of the G7 and G8 bases being "up".]

The contacts for band S2 are consistent with this adduct being the isomer in which the primary amine is located adjacent to the 5′ end of the GG strand. These included the contact detected between the ahaz NH_2 protons and G7 H8, T6 H6, and CH_3 in the $\tau_m = 150$ ms NOESY NMR spectrum together with the contacts between the T9 methyl group and proton 2 and the ligand endocyclic NH proton of the ahaz. These two protons are attached to chiral centers, and in this ligand orientation they point "down" relative to the platinum

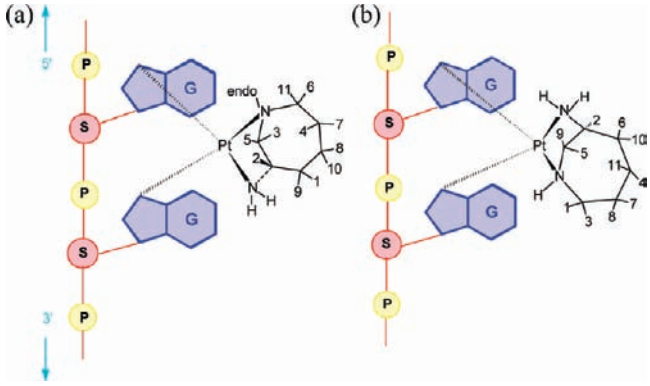

Figure 6. Ligand proton designations for (a) band S1 and (b) band S2.

Table 6. Ligand DNA Contacts for the S1 Isomer As Seen in the $\tau_m = 150$ ms NOESY Spectrum

ligand	DNA	r_{HH} (Å)
11	G7 H8	2.5−3.5
11	T6 H6	2.5−3.5
11	T6 3′	2.5−3.5
11	T6 5′	3.5−5
11	T6 4′	2.5−3.5
11	T6 1′	2.5−3.5
9	T6 2′	3.5−5
8	T6 CH_3	3.5−5
6	T6 CH_3	3.5−5
4	T6 H6	3.5−5
4	T6 CH_3	3.5−5
1	C21 NH4b	3.5−5
NH	G7 H8	3.5−5
NH	T6 2′	2.5−3.5
NH_2	G8 H8	3.5−5

plane, thereby allowing contact with the methyl protons of T9. To enable these contacts to be made, the base must be propeller-twisted underneath the ligand. The large upfield shift of the T9 methyl proton resonances is consistent with these ligand−DNA contacts and with the suggested arrangement of subelements of the structure. A section of the NOESY NMR spectrum ($\tau_m = 150$ ms) showing the ligand proton 2 in contact with T9 methyl group is presented in Figure 8.

The previously described molecular modeling studies carried out with the $\{Pt(S\text{-ahaz})\}^{2+}$ fragment bound to the central eight base pairs of the sequence indicated that the stereoisomer with the primary amine on the 5′ side of the adduct (now identified as band S2) is favored as it has few close contacts with the DNA, which is evident from the NMR spectra. This is consistent with the lesser degree of disruption to the duplex structure that is evidenced by such features as the smaller shifts of the G7 and G8 H8 resonances in the NMR spectra of band S2 and the maintenance of the sugar puckers in conformations typical of B-DNA for all nucleotides except G7.

Conclusions

The stereoselective bifunctional binding of the anticancer complex $[PtCl_2(S\text{-ahaz})]$ was investigated by reacting the complex with a purine-rich 14-mer oligonucleotide. HPLC methods were developed to separate the two isomeric products, only the fourth example to the best of our knowledge where separation of asymmetric platinum complexes attached to such an oligonucleotide has been achieved.[37−39] This is significant due to the close similarity of the HPLC separation properties of the two species. ESI mass spectrometry confirmed the identification of the separated components.

A detailed ^{1}H 2D NMR spectroscopic investigation of the two isomers allowed identification of the two HPLC bands through NOE correlations between the ahaz ligand and the 14-mer DNA duplex protons. The two isomeric platinated duplexes have contrasting structural differences: the minor isomer (band S1) identified on the basis of earlier molecular modeling studies was shown to cause greater disruption of the DNA duplex structure. The sugar ring of the 5′ bound guanine nucleotide adopts the C3′ endo pucker conformation characteristic of A-DNA in both isomers, a feature that has been observed in all previously determined structures of platinated duplex DNA. However, the minor isomer also causes the sugar ring associated with the nucleotide 5′ to the platinum adduct to adopt this pucker together with the sugar ring of the cytosine complementary to the 3′ side of the platinum lesion.

The ^{1}H NMR chemical shifts of the H8 resonances of the bound guanines also reflected the greater disruption to the

(37) Hartwig, J. F.; Lippard, S. J. *J. Am. Chem. Soc.* **1992**, *114*, 5646–5654.
(38) Kurosaki, H.; Tanaka, Y.; Sumimoto, M.; Goto, M. *J. Inorg. Biochem.* **1997**, *67*, 160.
(39) Dunham, S. U.; Dunham, S. U.; Turner, C. J.; Lippard, S. J. *J. Am. Chem. Soc.* **1998**, *120*, 5395–5406.

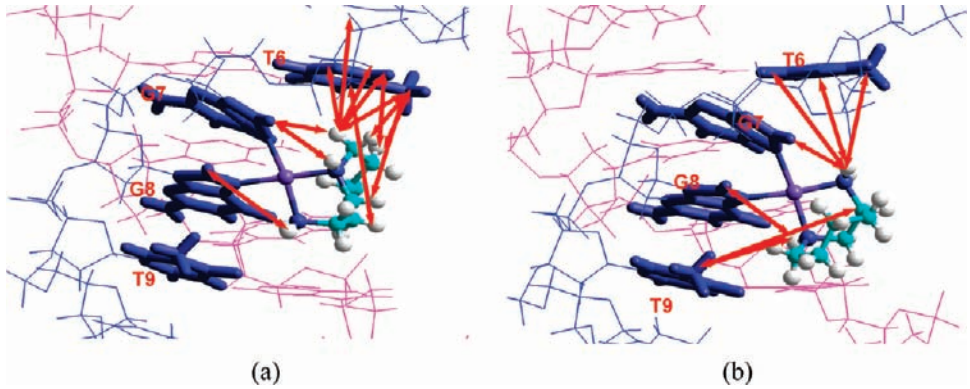

Figure 7. Molecular model illustrating the ligand−DNA contacts observed in the 150 ms NOESY spectrum of (a) band S1 and (b) band S2. The GG strand is in blue and the CC strand is in violet. These contacts are shown schematically in Supporting Information, Figure S8.

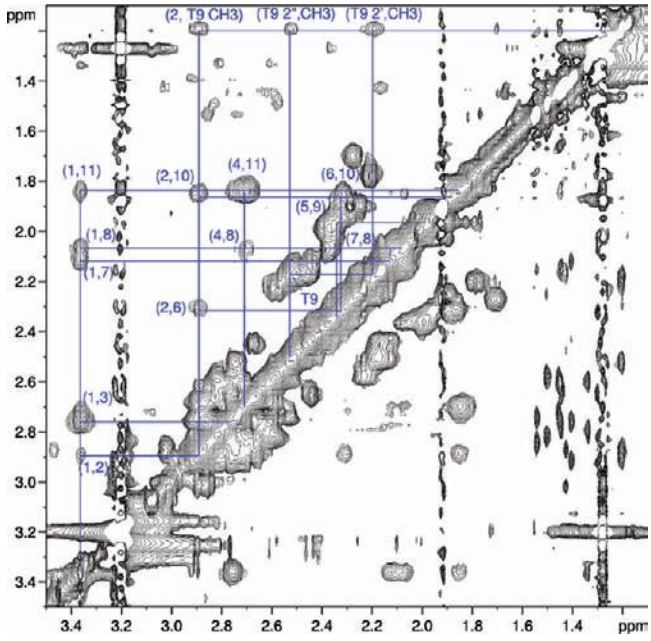

Figure 8. 2D NOESY NMR spectrum (τ_m =150 ms) showing the intraligand correlations and the correlation between ligand proton 2 and T9 CH_3 for band S2.

duplex by the minor isomer. Much larger deviations of the chemical shifts of the H8 resonances were observed when compared to those of the unplatinated 14-mer and the 14-mer with a cisplatin intrastrand adduct.[19] The major isomer was shown to have undergone structural changes in the DNA very similar to those observed for the cisplatin adducts.

This study, when combined with our previous studies, of the [$PtCl_2$(ahaz)] complexes[29−32] shows that the major determinant of their binding to duplex DNA is the steric bulk of the asymmetric ligand. This bulk has the ability to direct bifunctional adduct formation by facilitating or discouraging

Table 7. Ligand−DNA Contacts Leading to Determination of Isomer S2 Identification As Seen in the τ_m = 150 ms NOESY Spectrum

ligand	DNA	r_{HH} (Å)
2	T9 CH_3	3.5−5
NH_2	G7 H8	3.5−5
NH_2	G7 3′	2.5−3.5
NH_2	T6 H6	3.5−5
NH_2	T6 CH_3	3.5−5
NH	G8 H8	3.5−5
NH	T9 CH_3	3.5−5

ring closure from the monofunctional adducts, depending on the ligand orientation and chirality. Cytotoxicity studies show that the two enantiomers have similar activity, but in general the *R*-enantiomer is slightly more active.[29−32] This is surprising in the sense that the *R*-enantiomer forms only half as many intrastrand GpG adducts as the *S*-enantiomer. However, what this study shows is that low intrastrand adduct formation is correlated with higher distortion in the DNA, and it appears that this leads to higher cytotoxicity.

Acknowledgment. We thank Dr. Graham Ball (UNSW) for assistance with the 600 MHz NMR experiments. We thank the Australian Research Council and the Sydney University Cancer Research Fund for financial support, and the Cancer Council of NSW and the University of Sydney Travel Grants-in-Aid for funding for C.I.D.

Supporting Information Available: The HPLC chromatogram of the separated isomers and their ESI-MS spectra, the 1D NMR spectra obtained in formation of the duplex, 2D NOESY NMR spectrum used for stereospecific assignment of 2′, 2″ proton resonances, 2D NOESY NMR spectrum showing correlations used to confirm sugar puckers, variable temperature 1D NMR spectra of the imino proton resonance region, and 2D DQF-COSY NMR spectrum section showing ligand geminal pairs. This material is available free of charge via the Internet at http://pubs.acs.org.

IC802207M